Organic Geochemistry 147 (2020) 104081

Contents lists available at ScienceDirect

Organic Geochemistry

journal homepage: www.elsevier.com/locate/orggeochem

C_{41} methyl and C_{42} ethyl alkenones are biomarkers for Group II Isochrysidales

Sian Liao [a], Yuan Yao [b,c], Li Wang [d], Karen J. Wang [c], Linda Amaral-Zettler [c,e,f], William M. Longo [c], Yongsong Huang [c,*]

[a] *Department of Chemistry, Brown University, 324 Brook Street, Providence, RI 02912, USA*
[b] *Institute of Global Environmental Change, Xi'an Jiaotong University, Xi'an 710054, China*
[c] *Department of Earth, Environmental and Planetary Sciences, Brown University, 324 Brook Street, Providence, RI 02912, USA*
[d] *State Key Laboratory of Organic Geochemistry, Guangzhou Institute of Geochemistry, Chinese Academy of Sciences, Guangzhou 510640, China*
[e] *Department of Marine Microbiology and Biogeochemistry, NIOZ Royal Netherlands Institute for Sea Research and Utrecht University, P.O. Box 59, 1790 AB Den Burg, Texel, the Netherlands*
[f] *Department of Freshwater and Marine Ecology, Institute for Biodiversity and Ecosystem Dynamics, The University of Amsterdam, Amsterdam, the Netherlands*

ARTICLE INFO

Article history:
Received 2 May 2020
Received in revised form 22 June 2020
Accepted 6 July 2020
Available online 9 July 2020

Keywords:
C_{41} and C_{42} alkenones
Biomarkers
Isochrysidales
Culture
Evolution
18S rDNA

ABSTRACT

Alkenones are polyunsaturated long-chain methyl or ethyl ketones produced by species in the Isochrysidales, an order of haptophyte algae. Based on phylogenetic data, members of the Isochrysidales have been classified into three groups with each group showing significant differences in alkenone profiles and preferred growth environments. Common carbon chain lengths of alkenones range from 37 to 40. Extended C_{41} methyl (C_{41}Me) and C_{42} ethyl (C_{42}Et) alkenones have been reported in hypersaline lakes in China (Lake Alahake and Lake Balikun), Canada (Lake Snakehole) and marine sediments (e.g., ~95 Ma in Blake-Bahama Basin). It is unclear, however, if these extended alkenones are produced by one or more groups of Isochrysidales. Here, we systematically examined alkenones from cultures of Group II (*Isochrysis nuda*, *Isochrysis litoralis*, *Ruttnera lamellosa*, *Isochrysis galbana* and *Tisochrysis lutea*) and Group III (*Emiliania huxleyi* and *Gephyrocapsa oceanica*) Isochrysidales and environmental samples of Group I Isochysidales. C_{41}Me and C_{42}Et alkenones were found in all Group II species with *Isochrysis nuda* producing the highest percentages, but not in alkenones produced by Group I nor Group III Isochrysidales. Our results indicate that extended C_{41}Me and C_{42}Et alkenones are specific biomarkers for Group II Isochrysidales. We also report the first temperature calibrations of alkenones for *Isochrysis nuda* and *Isochrysis litoralis* using culture experiments, and find temperatures inferred from extended alkenones in Balikun and Alahake surface sediments match warm-season temperatures based on *Isochrysis nuda* calibrations, which is further corroborated by genomic data indicating the dominance of *Isochrysis nuda* Isochrysidales.

1. Introduction

Alkenones are a class of polyunsaturated long-chain ketones produced by the Isochrysidales, an order of haptophyte algae (Volkman et al., 1980; Conte et al., 1998; Versteegh et al., 2001; D'Andrea and Huang, 2005; Nakamura et al., 2016; Zheng et al., 2016, 2019). Because of the strong pseudo-linear response between the unsaturation degrees of alkenones and environmental temperature, alkenones are of particular interest to paleoclimatologists and paleoceanographers, and have been widely used for paleo-sea surface temperature (SST) reconstructions in the past 40 years (Brassell et al., 1986; Prahl and Wakeham, 1987; Rosell-Melé and Comes, 1999; Bendle and Rosell-Melé, 2007; Tzanova and Herbert, 2015).

Common alkenones found in culture and sediment samples contain 37 to 40 carbon atoms in a straight alkyl chain. C_{41}Me and C_{42}Et alkenones with extended-chain lengths were first reported in the Cretaceous marine sediment sample from the Blake-Bahama Basin (~95 Ma) (Farrimond et al., 1986). Only di-unsaturated alkenones including C_{41}Me ($C_{41:2}$Me) and C_{42}Et ($C_{42:2}$Et) were reported, possibly because of the high temperature during the Cretaceous period or the lack of biosynthesis pathway in ancient alkenone producers to produce tri-unsaturated alkenones (Brassell, 2014; O'Brien et al., 2017). Both tri- and

---

* Corresponding author.
E-mail address: yongsong_huang@brown.edu (Y. Huang).

https://doi.org/10.1016/j.orggeochem.2020.104081
0146-6380/

di- unsaturated C_{41}Me and C_{42}Et alkenones were reported in surface sediment samples from hypersaline Lake Alahake and Lake Balikun in China (Zhao et al., 2014). Double bond positions in $C_{41:3}$Me and $C_{42:3}$Et alkenones, determined using dimethyl disulfide (DMDS) adduction reaction, were found to be Δ^7, Δ^{14}, Δ^{21} (numbering from the carbonyl carbon), the same as common tri-unsaturated C_{37} to C_{39} alkenones (Longo et al., 2013; Zhao et al., 2014; Dillon et al., 2016). In marine sediments from Punta Grande/Punta Piccola sections (2.6–3.6 Ma), extended C_{41} alkenones were detected after $NaBH_4$ reduction and silylation (Plancq et al., 2015). C_{41}Me and C_{42}Et alkenones were then reported in a Canadian hypersaline lake, Lake Snakehole (Araie et al., 2018). An Isochrysidales strain (named *Sh 1*) was subsequently isolated from Lake Snakehole and found to produce these extended alkenones in culture experiments. Recently, di-unsaturated C_{41}Me and C_{42}Et alkenones were also reported in sediment sample from Bass River (~41 Ma) by de Bar et al. (2019). Marine haptophytes were proposed as the corresponding alkenone producers.

Despite this progress, it is unclear if C_{41}Me and C_{42}Et alkenones are exclusively produced by phylogenetically closely related species or distantly related species (or groups) of Isochrysidales. The Isochrysidales has been divided into three distinct groups based on phylogenetic data (Theroux et al., 2010): Group I Isochrysidales are typically found in freshwater and oligohaline environments (Longo et al., 2016, 2018; Wang et al., 2019a,2019b; Yao et al., 2019), Group II Isochrysidales in coastal seas and brackish to hypersaline lacustrine environments (Theroux et al., 2010; Randlett et al., 2014; Zhao et al., 2014; Araie et al., 2018; Kaiser et al., 2019) and Group III Isochrysidales in open ocean areas (Brassell et al., 1986; Müller et al., 1998; Harada et al., 2003; Longo et al., 2016; Zheng et al., 2019). Based on small and large subunit rRNA gene phylogenetic reconstructions, strain *Sh 1* isolated from Lake Snakehole was classified as a Group II Isochrysidales, closely related to *Isochrysis nuda* strains (RCC1207, AC49, and PLY401b) and *Isochrysis litoralis* strains (AC18, RCC1346) (Araie et al., 2018). However, extended C_{41}Me and C_{42}Et alkenones have also been reported in marine sediment samples from the Blake-Bahama Basin (Farrimond et al., 1986), Punta Grande/Punta Piccola sections (Plancq et al., 2015) and Bass River (de Bar et al., 2019). It is therefore unclear whether Group III (or even Group I) Isochrysidales can produce C_{41}Me and C_{42}Et alkenones.

The relatively rare reports of extended-chain C_{41}Me and C_{42}Et alkenones may reflect the low abundance of these compounds, and the use of conventional non-polar gas chromatography (GC) columns. Longo et al. (2013) and Zheng et al. (2017) have shown that, when a mid-polar GC column with trifluoropropylmethylsiloxane stationary phase was used, alkenones had significantly shorter retention times and higher peak resolutions for methyl and ethyl alkenones, relative to when a non-polar GC column with polydimethylsiloxane stationary phase was used. Therefore, the use of mid-polar GC columns could have contributed to recent discoveries of the relatively high molecular weight C_{41}Me and C_{42}Et alkenones in saline lakes (Zhao et al., 2014; Araie et al., 2018).

Here, we systematically examined alkenone profiles in different Isochrysidales groups to determine if the extended-chain C_{41}Me and C_{42}Et alkenones are produced by one or more groups of Isochrysidales. A mid-polar GC column RTX-200 was used to ensure the best detection of extended-chain alkenones (Zheng et al., 2017). We also conducted the first culture-based temperature calibration of *I. nuda* and *I. litoralis*, and performed analysis and 18S rRNA gene sequencing on our newly collected sediment samples from Lake Balikun and Lake Alahake, known to contain extended-chain C_{41}Me and C_{42}Et alkenones.

2. Materials and methods

2.1. Culture experiments

Six Isochrysidales species were purchased from various algal culture collections: *I. litoralis* (AC18) from the Algobank-Caen, *I. nuda* (RCC1207) and *Gephyrocapsa oceanica* (RCC3483) from the Roscoff Culture Collection, *Emiliania huxleyi* (NIES1312) from the National Institute for Environmental Studies, *E. huxleyi* (CCMP2090) from the National Center for Marine Algae and Microbiota and *Tisochrysis lutea* (UTEX LB 2307) from the Culture Collection of Algae at The University of Texas at Austin. *T. lutea* (UTEX LB 2307) was originally named as *Isochrysis aff. galbana* (UTEX LB 2307), but then reassigned as *T. lutea* (UTEX LB 2307) based on phylogenetic analysis (Bendif et al., 2013; Nakamura et al., 2016).

Culture growth and harvest procedures were similar to those reported in Zheng et al. (2016, 2019), but with small modifications. All six species were acclimatized for about two weeks before the start of the corresponding culture experiments with f/2 medium (Guillard, 1975). *I. nuda* (RCC1207) and *I. litoralis* (AC18) were cultured at 4, 10, 15, 20 and 25 °C, *E. huxleyi* (NIES1312) at 9 and 15 °C, *G. oceanica* (RCC3483) at 18 °C. f/2 medium for these four species was prepared from seawater collected from Vineyard Sound, Woods Hole, MA, USA at a salinity of 32 ppt (filtered using 0.2 μm Whatman nylon membrane filter and then autoclaved). To investigate the effect of reduced nutrients, *I. nuda* (RCC1207) and *I. litoralis* (AC18) were cultured at 15 °C with f/20 medium which is diluted by ten times from f/2 medium with filtered seawater. Cultures were grown under a light:dark cycle set at 16:8. The light intensity was 140 $\mu E\ m^{-2}\ s^{-1}$ except for *E. huxleyi* (NIES1312) whose light intensity was 17 $\mu E\ m^{-2}\ s^{-1}$. Cultures experiments were performed in 165 ml medium at the growth chamber facility administrated by the Institute at Brown for Environment and Society, Brown University, USA. *E. huxleyi* (CCMP2090) *and T. lutea* (UTEX LB 2307) were grown at 20 and 25 °C, respectively, with autoclaved f/2 medium prepared from seawater collected from the South China Sea, China at a salinity of 32 ppt (filtered using 0.2 μm Whatman cellulose filter). Cultures were grown under a light:dark cycle set at 12:12. The light intensity was 40 $\mu E\ m^{-2}\ s^{-1}$. Cultures experiments were performed in 200 ml medium at the Guangzhou Institute of Geochemistry, Chinese Academy of Sciences, China.

Cultures were harvested at early stationary phase (monitored using hemocytometer counts (Hausser Scientific, PA, USA)) by filtering onto 0.7 μm glass fiber filters (Merck Millipore, MA, USA). All filters were wrapped with aluminum foils and immediately frozen at −20 °C for further extraction and analysis (Zheng et al., 2016).

To obtain additional alkenone profiles from a diversity of Isochrysidales species, we concentrated and re-examined previously characterized culture samples including *Ruttnera lamellosa* (CCMP1307), *Isochrysis galbana* (CCMP1323), *T. lutea* (CCMP463) and *E. huxleyi* (Van556) (Zheng et al., 2019). Because there is currently no culture of a Group I haptophyte species available, surface sediment samples from Lake Braya Sø in Greenland, Lake White Fish and Lake Devil Mountain in Alaska, and suspended particulate matter samples from Toolik Lake in Alaska were re-analyzed to represent alkenone profiles for Group I species (Longo et al., 2016; Wang et al., 2019a,2019b).

2.2. 18S rDNA analysis of sediment samples from Lake Balikun and Lake Alahake, China

New surface sediment samples from Lake Balikun (43.662°N, 92.825°E) and Lake Alahake (47.684°N, 87.572°E) were collected in the summer of 2017. These lakes have been reported to contain

C_{41}Me and C_{42}Et alkenones (Zhao et al., 2014). Monthly air temperature data (1970–2000) was extracted from the WorldClim-Global Climate Database (http://www.worldclim.org /version2; Fick and Hijmans, 2017) with 30 s (~1 km^2) spatial resolution. Samples for DNA extraction were frozen at −80 °C in the laboratory until analysis. Procedures for DNA extraction, amplification, cloning and sequencing of DNA followed Yao et al. (2019). DNA was extracted from ~0.5 g sediment subsamples using the FastDNA SPIN Kit (MP Biomedicals, OH, USA) according to the manufacturer's instructions. The main processes include cell lysis, removal of proteins, and purification of DNA. DNA concentrations were quantified by measuring optical absorbance at 260 nm using a NanoDrop ND-1000 spectrophotometer (Thermo Scientific, Wilmington, USA). The haptophyte-specific oligonucleotide primers (Prym-429F, Prym-887R) were used for the amplification of targeted 18S rDNA (Coolen et al., 2004). PCR reactions (25 µl volume) contained 16.2 µl double distilled water, 2.5 µl 10 × buffer (TaKaRa Bio, Otsu, Japan), 2 µl dNTP (2.5 mM, TaKaRa Bio, Otsu, Japan), 2 µl a pair of primers (10 µM), 1 µl bovine serum albumin (BSA, 20 mg/ml, TaKaRa Bio, Otsu, Japan), 0.3 µl Ex Taq (5 U/µl, TaKaRa Bio, Otsu, Japan), and 1 µl template sample. All reactions were performed using the following conditions: 4 min initial denaturing at 96 °C, followed by 35 cycles including denaturing (30 s at 94 °C), primer annealing (40 s at 55 °C), and primer extension (40 s at 72 °C), with a final extension of 10 min at 72 °C (Coolen et al., 2004). The PCR amplified 18S rDNA of haptophytes (463 bp) was separated by agarose gel electrophoresis and was then purified using the Nucleic Acid Purification Kit (Axygen, NY, USA) according to the manufacturer's instructions. The purified DNA was cloned with pGEM-T Easy Vector (Promega, WI, USA) and DH5α competent cells according to the manufacturer's instructions. Finally, the cells transformed with vectors containing recombinant DNA (white colonies) using the blue-white screen were sequenced. A blank control was included in all of the above steps, which serves as a control for cross-contamination during the experiments.

All obtained DNA sequences were analyzed as queries in Basic Local Alignment Search Tool (BLAST) searches against the National Center for Biotechnology Information (NCBI) database (http://blast.ncbi.nlm.nih.gov/Blast.cgi) with default parameters and were then removed vector sequences. The operational taxonomic units (OTUs) of all trimmed sequences were determined using the DOTUR software program with a 98% cut-off criterion (Schloss and Handelsman, 2005). The representative sequences from each OTU were used to construct a phylogenetic tree along with some haptophyte DNA sequences from the public GenBank database. The neighbor-joining tree was constructed using the molecular evolutionary genetics analysis (MEGA) software with 1000 bootstrap replications. Representative sequences for each OTU in this study have been deposited in GenBank (Accession numbers MT373478-MT373480).

2.3. Analysis of alkenones and alkenoates

Filters of *I. nuda* (RCC1207), *I. litoralis* (AC18), *E. huxleyi* (NIES1312) and *G. oceanica* (RCC3483) were freeze-dried overnight and then sonicated three times with dichloromethane (DCM, 3 × 30 min, 40 ml each time) for lipid extractions. Total extracts were divided into three fractions using silica gel (230–400 mesh, 40–63 µm) in glass pipettes, and eluted with hexane, DCM and methanol. Alkenones and alkenoates were in the DCM fraction. Sediment samples from Lake Balikun and Lake Alahake were further purified with silver-thiolate columns to remove co-elution compounds and get cleaner chromatograms (Wang et al., 2019a,2019b). All culture extracts including *I. nuda* (RCC1207), *I. litoralis* (AC18), *R. lamellosa* (CCMP1307), *I. galbana* (CCMP1323), *T. lutea* (CCMP463), *E. huxleyi* (Van556), *E. huxleyi* (NIES1312) and *G. oceanica* (RCC3483) as well as samples from Lake Balikun, Lake Alahake, Lake Braya Sø, Lake White Fish, Lake Devil Mountain and Toolik Lake were then analyzed by GC-FID (Agilent 7890B) and GC–EI-MS (Agilent 7890B interfaced to 5977 inert plus MSD) equipped with RTX-200 columns (105 m × 250 µm × 0.25 µm film thickness) (Zheng et al., 2017). 18-Pentatriacontanone was used as an internal standard. For the analysis on GC-FID, the carrier gas was hydrogen. Samples were injected under pulsed splitless mode at 320 °C. The initial pulse pressure was 35 psi for the first 1 min. Then the purge flow to split vent was 35.0 ml/min at 1.1 min. The flow rate (constant flow mode) was 1.5 ml/min. The initial oven temperature was 50 °C for 2 min, then increased to 255 °C at 20 °C/min, then increased to 320 °C at 3 °C/min and held for 35 min. For the analysis by GC–EI-MS, samples were injected under pulsed splitless mode at 320 °C. The initial pulse pressure was 35 psi for the first 0.5 min. The purge flow to split vent was 50 ml/min at 1.1 min. The flow rate (constant flow mode) was 1.6 ml/min. The initial oven temperature was 40 °C for 1 min, then increased to 255 °C at 20 °C/min, then increased to 315 °C at 3 °C/min and held for 35 min. Samples were analyzed under full-scan mode. The source temperature was 230 °C. The electron ionization energy was 70 eV. The mass range was from *m/z* 50 to 650. GC-FID and GC–MS analyses were performed at the Department of Earth, Environmental and Planetary Sciences, Brown University, USA. Filters of *E. huxleyi* (CCMP2090) *and T. lutea* (UTEX LB 2307) were analyzed at the Guangzhou Institute of Geochemistry, Chinese Academy of Sciences, China, following similar analytical protocols as those analyzed at Brown University.

All alkenone and alkenoate indices were based on literature definitions and are as follows (Araie et al., 2018; Zheng et al., 2019):

$$U^{m}_{n} = (C_{n:2} - C_{n:4})/(C_{n:2} + C_{n:3} + C_{n:4}) \tag{1}$$

$$U^{m'}_{n} = C_{n:2}/(C_{n:2} + C_{n:3}) \tag{2}$$

$$U^{m''}_{n} = C_{n:3}/(C_{n:3} + C_{n:4}) \tag{3}$$

$$RIE_{36E} = C_{36:3a}OEt/(C_{36:3a}OEt + C_{36:3b}OEt) \tag{4}$$

For alkenone indices, m is K (ketone) and n is the number of carbon atoms in the ketone chain and could be 37 to 42. For example, $C_{37:2}$ is the abundance of an alkenone with 37 carbon atoms and two C = C double bonds. For alkenoate indices, m is E (ester) and n is the number of carbon atoms in the carboxylic acid chain and is 36. 3_a and 3_b are tri-unsaturated double bond positional isomers (Longo et al., 2013). For example, $C_{36:3a}$OEt and $C_{36:3b}$OEt are abundances of two ethyl alkenoates with 36 carbon atoms in the carboxylic acid chain and three C = C bonds but with double bond positions located at Δ^7, Δ^{14}, Δ^{21}, and Δ^{14}, Δ^{21}, Δ^{28} respectively.

2.4. Quantification of C_{41}Me and C_{42}Et alkenones

C_{41}Me and C_{42}Et alkenones were identified based on comparison of retention times on GC-FID with well-characterized Greenland lake alkenones and mass spectra on GC–MS (Supplementary Fig. S1). Because of the relatively low abundances of C_{41}Me and C_{42}Et alkenones, the amount of C_{41}Me and C_{42}Et alkenones was expressed as ratios relative to the total amount of C_{37}Me alkenones unless otherwise specified. Accurate quantification of C_{41}Me and C_{42}Et alkenones and calculation of $U^{K'}_{41}$ and $U^{K'}_{42}$ values require concentrating corresponding alkenone samples. At very low alkenone concentrations (<0.25 ng), analytical errors of C_{41}Me alkenones increased (Supplementary Fig. S2). This problem may largely originate from the non-linear response of different alkenones at the extremely low concentrations. However, we found that when the amount of $C_{41:3}$Me alkenone on the GC-FID was above 0.25 ng, $U_{41}^{K'}$ values were quite constant with a maximum error of ∼±0.1 °C for inferred temperatures. By concentrating samples, we ensured that the smallest amounts of $C_{41:3}$Me alkenone injected into the GC-FID for all culture and sediment samples were > 0.4 ng, which corresponded to a maximum error of ∼± 0.1% for C_{41}/C_{37}% (Supplementary Fig. S2b, Supplementary Table S1). In order to reduce the quantification error due to the peak shape distortion, each sample was injected twice on the GC-FID with two levels of concentrations (Supplementary Table S1). We first determined the ratios of $C_{39:3}$Me and $C_{40:3}$Et over C_{37} alkenones in a relatively dilute solution (C_{37} alkenone peak shapes were not distorted). We then concentrated samples to determine the ratios of C_{41}Me and C_{42}Et over $C_{39:3}$Me and $C_{40:3}$Et alkenones. The data were combined to obtain accurate ratios of C_{41}Me/C_{42}Et alkenones over C_{37}Me alkenones.

3. Results and discussion

3.1. C_{41}Me and C_{42}Et alkenones as biomarkers for Group II Isochrysidales

We found C_{41}Me and C_{42}Et alkenones in cultures of all five Group II species including *I. nuda*, *I. litoralis*, *R. lamellosa*, *I. galbana* and *T. lutea,* with concentrations ranging from 0.038% to 2.0% relative to C_{37} alkenones (Fig. 1, Supplementary Table S1). Based on LSU (large subunit) and SSU (small subunit) ribosomal RNA phylogenies, *I. nuda* and *I. litoralis* are closely related to the known C_{41}Me/C_{42}Et producers *Sh 1* (Araie et al., 2018). *R. lamellosa*, *I. galbana* and *T. lutea* are more distantly related but were also found to produce C_{41}Me and C_{42}Et alkenones (Fig. 1a–e). We didn't find C_{41}Me and C_{42}Et alkenones in Group I as represented by sediment samples from Lake Braya Sø, Lake White Fish, Lake Devil Mountain and five suspended particulate matter samples from Toolik Lake nor in all culture samples of Group III species examined (Fig. 1g–k). Collectively, our results indicate that C_{41}Me and C_{42}Et alkenones are biomarkers for Group II Isochrysidales.

Discovery of Group II-specific biomarkers is important for assessing mixed alkenone contributions from Group II and III Isochrysidales in (marginal) marine sediments. Such mixed production has previously been identified in Baltic Sea regions based on both alkenone profiles and DNA sequencing results (Kaiser et al., 2019), and could complicate corresponding temperature reconstructions (Wang et al., 2019a,2019b; Zheng et al., 2019). In our previous culture studies, the longest alkenones we found in Group II species were C_{40}Et alkenones which were proposed as an indicator for Group II Isochrysidales (Kaiser et al., 2019; Zheng et al., 2019). However, as we concentrated our samples in search of C_{41}Me and C_{42}Et alkenones in the current study, we found C_{40}Et alkenones in samples of all three groups of Isochrysidales with lower percentages in Group I and Group III than in Group II Isochrysidales (Fig. 1, Supplementary Table S1). Hence C_{41}Me and C_{42}Et are more suitable biomarkers than C_{40}Et for identifying the alkenone production from Group II species in mixed systems.

3.2. Effects of species, temperature and nutrient level on the production of C_{41}Me and C_{42}Et alkenones in Group II Isochrysidales

Percentages of C_{41}Me and C_{42}Et relative to C_{37} alkenones varied among different Group II species (Fig. 2a). On average, *I. nuda* contained the highest percentage of C_{41}Me and C_{42}Et (1.0%), followed by *R. lamellosa* (0.27%), *T. lutea* (0.26%), *I. litoralis* (0.20%) and *I. galbana* (0.11%). For *I. nuda*, no clear trend between temperature and relative abundances of C_{41}Me and C_{42}Et over C_{37}Me alkenones was observed (Fig. 2b). Relative percentages of C_{41}Me and C_{42}Et over C_{37}Me alkenones at 10 °C and 15 °C were similar and lower than those at 4, 20 and 25 °C. For *I. litoralis*, however, there was a decreasing trend in C_{41}Me and C_{42}Et percentages over C_{37}Me alkenones from 4 °C to 20 °C, except at 25 °C. We performed only one set of growth experiments at 15 °C for *I. nuda* and *I. litoralis* at two different levels of nutrient conditions using f/2 and f/20 growth mediums. In both species, changes from f/2 to f/20 culture medium increased the relative production of C_{41}Me and C_{42}Et alkenones by 403% for *I. nuda* and by 146% for *I. litoralis*. Our preliminary results suggest that the production of C_{41}Me and C_{42}Et alkenones might increase under lower nutrient conditions, but more experimental data are needed to validate this potential nutrient effect.

Unlike other Group II species, C_{41}Me and C_{42}Et alkenones were only found in *T. lutea* (CCMP463) grown at 25 °C, but not at 4, 14 and 20 °C. *T. lutea* is morphologically similar to *I. galbana* and was once named as "*Isochrysis* aff. *galbana* clone T-iso". It was later reassigned to a new Group II genus and species based on the phylogenetic analyses (Bendif et al., 2013; Nakamura et al., 2016). However, based on the overall alkenone and alkenoate distributions (Zheng et al., 2019), *T. lutea*'s alkenone profiles seem to display certain Group III characteristics compared with other Group II species. For example, *T. lutea* produces little $C_{37:4}$ alkenone even at relatively low growth temperatures (Zheng et al., 2019), which is a feature more commonly observed in Group III Isochrysidales. Moreover, the correlation of unsaturation ratios with temperature in *T. lutea* is similar to Group II Isochrysidales above 15 °C, but more similar to *E. huxleyi* at lower temperatures, suggesting that temperature may control different biosynthetic outcomes (Zheng et al., 2019). Based on these observations, Zheng et al. (2019) suggested that *T. lutea* could be an intermediate species between Group II and Group III Isochrysidales in terms of alkenone production. Therefore, the occurrence of extended alkenones only at higher growth temperature (25 °C) in *T. lutea* (CCMP463) may reflect an increased expression of Group II-type biosynthesis pathways for these extended alkenones. Importantly, however, we didn't find C_{41}Me and C_{42}Et alkenones in another *T. lutea* strain (UTEX LB 2307) cultured at 25 °C. This might indicate that different strains of *T. lutea* differ in the temperature threshold for the production of C_{41}Me and C_{42}Et alkenones.

3.3. Rationalization for the production of C_{41}Me and C_{42}Et alkenones in Group II Isochrysidales

The production of C_{41}Me and C_{42}Et alkenones in Group II Isochrysidales is not entirely unexpected based on the characteristic differences in alkenone and alkenoate profiles for different groups of Isochrysidales (Zheng et al., 2019). Specifically, both Group I and III Isochrysidales produce C_{38}Me and C_{39}Et alkenones. However, Group II Isochrysidales do not make, or make only a trace amount of, C_{38}Me and C_{39}Et alkenones. Alkenones and related alkenoates are produced by Isochrysidales possibly as carbon storage for energy (Epstein et al., 2001; Shi et al., 2015; Bakku et al., 2018). Thus, we hypothesize that the production of extended-chain C_{41}Me and C_{42}Et alkenones in Group II Isochrysidales may help compensate, from an energy conservation point of view, for the lack of the shorter chain C_{38}Me and C_{39}Et alkenones. The exact biosynthetic mechanism requires further study, involving identifying the specific genes responsible for alkenone production in different groups of Isochrysidales.

3.4. Evolution of Group II and Group III alkenone biosynthesis genes

Our current understanding of alkenone characteristics for different groups of Isochrysidales gives us an opportunity to discuss the evolution of alkenone biosynthesis genes from the perspective of their alkenone profiles. C_{41}Me and C_{42}Et alkenones were first

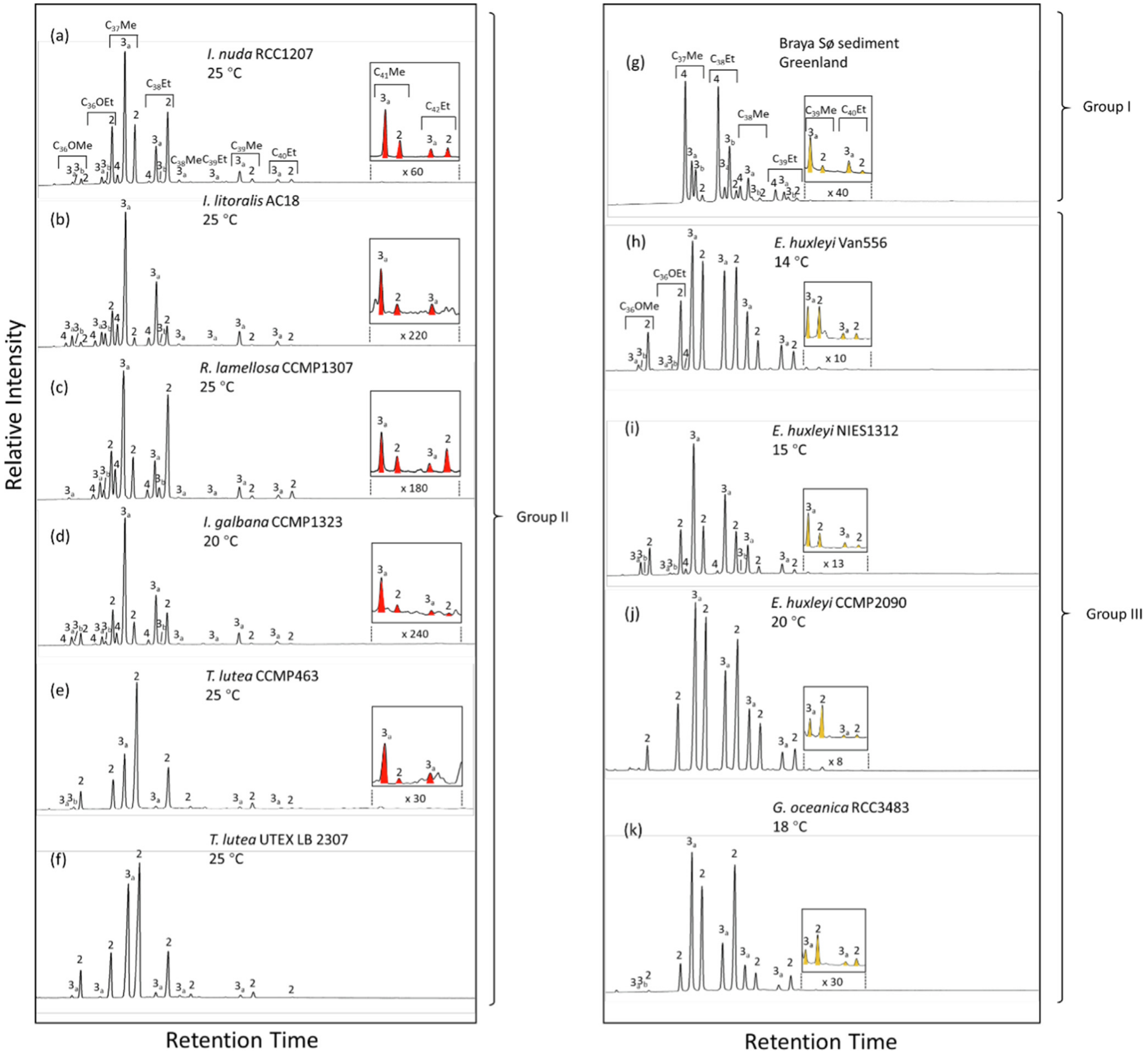

Fig. 1. Gas chromatograms showing the distribution of alkenones and alkenoates for different groups of Isochrysidales. Group II samples include culture samples of *I. nuda* (RCC1207) (a), *I. litoralis* (AC18) (b), *R. lamellosa* (CCMP1307) (c), *I. galbana* (CCMP1323) (d), *T. lutea* (CCMP463) (e) and *T. lutea* (UTEX LB 2307) (f). Lake Braya Sø sediment sample shows representative alkenone profiles for Group I species (g). Group III samples include culture samples of *E. huxleyi* (Van556) (h), *E. huxleyi* (NIES1312) (i), *E. huxleyi* (CCMP2090) (j) and *G. oceanica* (RCC3483) (k). Numbers above each peak are the number of C=C bonds in corresponding compounds. C_{41}Me and C_{42}Et alkenones are highlighted with red color in corresponding Group II culture samples, which were reinjected into the GC after concentrating the solution (Supplementary Table S1). C_{39}Me and C_{40}Et alkenones are highlighted with yellow in samples of Group I and Group III Isochrysidales, which were reinjected into the GC after concentrating the solution (Supplementary Table S1). (For interpretation of the references to color in this figure legend, the reader is referred to the web version of this article.)

reported in a sediment sample from Blake-Bahama Basin (~95 Ma, Deep Sea Drilling Project (DSDP), Leg 76) (Farrimond et al., 1986). The presence of these extended alkenones suggests that alkenones in the Blake-Bahama Basin were likely produced by Group II-like species. We also note the oldest alkenones reported so far are from Lower Aptian porcellanite (~120.5 Ma) deposited during oceanic anoxic event (OAE) 1a (Ocean Drilling Program (ODP), Leg 198, Shatsky Rise). These Lower Aptian alkenone distributions seem to display Group II alkenone characteristics showing the presence of C_{37}Me, C_{38}Et, C_{39}Me and absence of C_{38}Me and C_{39}Et alkenones (Brassell et al., 2004). No C_{41}Me and C_{42}Et alkenones were detected in lower Aptian porcellanite, possibly because of low abundances or detection problems during gas chromatographic analysis (GC chromatograms display significant co-elutions; Brassell et al., 2004). $C_{40:2}$Et-dominant alkenone profiles reported in sediments from Geulhemmerberg (~66 Ma) (Yamamoto et al., 1996) and Bass River (~78 Ma, ODP, Leg 174, New Jersey Coastal Plain; de Bar et al., 2019) are less consistent with typical Group II alkenone profiles. However, we observe in contemporary Isochrysidales that C_{40}Et alkenones are in general produced in larger quantity by Group II species than by other groups of Isochrysidales. For example, Group II species generally have six times higher percentages of C_{40}Et/C_{37}Me than Group III species and two times higher percentages than Group I species (Supplementary Table S1). Therefore, an exceptionally high abundance of $C_{40:2}$Et alkenones may also indicate the expression of Group II alkenone biosynthesis genes. In

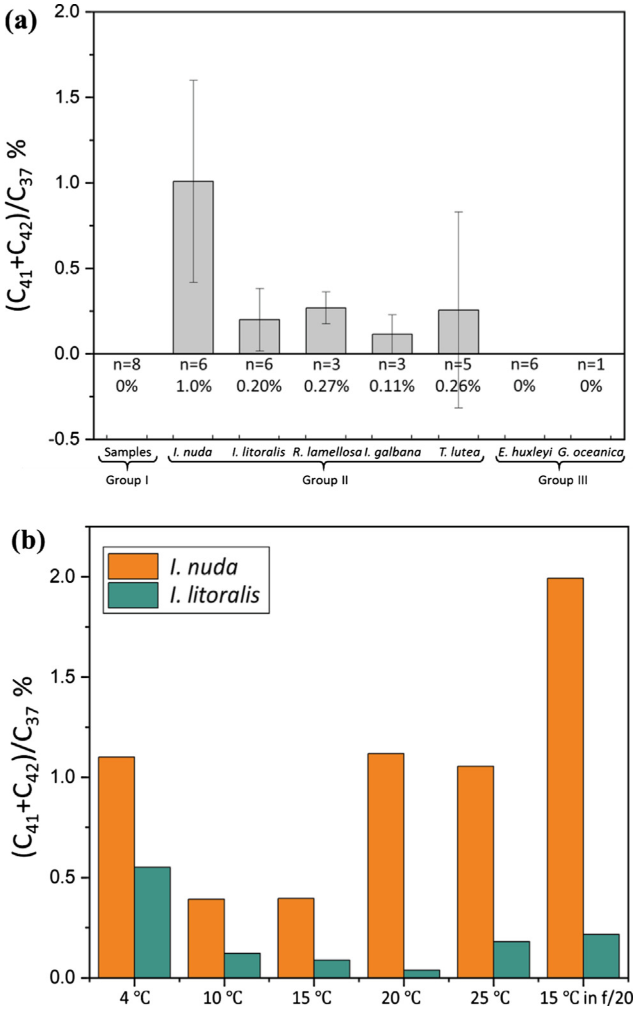

Fig. 2. (a) Average ratios of C_{41}Me and C_{42}Et alkenones over C_{37} alkenones in Group I, Group II and Group III samples; n is the number of samples examined. Group I samples (n = 8) include surface sediment samples from Lake Braya Sø in Greenland (D'Andrea et al., 2006), Lake White Fish and Lake Devil Mountain in Alaska (Wang et al., 2019a) and five suspended articulate matter samples (at depths of 1 m, 2 m, 3 m, 5 m, 8 m) from Toolik Lake in Alaska (Longo et al., 2016). Group II samples include culture samples of *I. nuda* (RCC1207 cultured at 4, 10, 15, 20, 25 °C with f/2 growth medium, and 15 °C with f/20 medium), *I. litoralis* (AC18 cultured at 4, 10, 15, 20, 25 °C with f/2 growth medium, and 15 °C with f/20 medium), *R. lamellosa* (CCMP1307 cultured at 4, 20, 25 °C), *I. galbana* (CCMP1323 cultured at 9, 20, 25 °C), *T. lutea* (CCMP463 cultured at 4, 14, 20, 25 °C and UTEX LB 2307 cultured at 25 °C). Group III samples include culture samples of *E. huxleyi* (Van556 cultured at 9, 14, 20 °C, NIES1312 cultured at 9, 15 °C and CCMP2090 cultured at 20 °C) and *G. oceanica* (RCC3483 cultured at 18 °C). (b) Ratios of C_{41}Me and C_{42}Et alkenones relative to C_{37} alkenones in culture samples of *I. nuda* (RCC1207) and *I. litoralis* (AC18) at temperatures ranging from 4 to 25 °C in f/2 medium, and at 15 °C in f/20 medium.

contrast, alkenones in sediments from the central Arctic Ocean (~49 Ma, Integrated Ocean Drilling Program (IODP), Expedition 302) and Bass River (~50 Ma) seem to display distribution pattern of Group III-like species, with the presence of both methyl and ethyl ketones for C_{38} alkenones (Weller and Stein, 2008; de Bar et al., 2019). Coccolith fossils of contemporary marine type (Group III) Isochrysidales *E. huxleyi* and *G. oceanica* only appeared 0.291 Ma and 1.85 Ma ago, respectively (Pujos-Lamy, 1977; Raffi et al., 2006; de Bar et al., 2019). Collectively, these alkenone profiles (and fossil records) suggest that Group II alkenone biosynthesis genes may have evolved much earlier than Group III genes. This hypothesis is, to a certain extent, consistent with the phylogenetic analysis based on LSU and SSU rRNA conducted by Richter et al. (2019) which showed that Group II Isochrysidales branch earlier than other groups of Isochrysidales.

The occurrence of Group III-type alkenone profiles (presence of both C_{38}Et and C_{38}Me alkenones) generally coincides with the first occurrence of tri-unsaturated alkenones (~49 Ma, central Arctic Ocean) after the Early Eocene Climatic Optimum (EECO) with a significant decrease in SST (Weller and Stein, 2008; Brassell, 2014). This indicates that certain environmental factors (e.g., cooling temperature) might have facilitated the evolution of biosynthesis pathways for C_{38}Me and tri-unsaturated alkenones (Brassell, 2014), and occurrence of Group III Isochrysidales. The possible correlation between cooling temperature and occurrence of Group III Isochrysidales seemingly also relates to the phenomenon that changes in unsaturation ratios for *T. lutea*, proposed as an intermediate species between Group II and Group III species, are more similar to those of Group III species *E. huxleyi* at low temperatures (Zheng et al., 2019).

We note that the alkenone profile in Bass River (~41 Ma) displays an unusual pattern with the presence of C_{37}Me, C_{38}Et, C_{38}Me, C_{39}Et, C_{39}Me, C_{40}Et, C_{41}Me and C_{42}Et alkenones. Marine haptophytes were proposed as corresponding alkenone producers (de Bar et al., 2019). The presence of both C_{38}Et and C_{38}Me alkenones indicates the contribution from Group III Isochrysidales or biosynthesis genes. However, our data demonstrate that the presence of C_{41}Me and C_{42}Et alkenones (and the relatively high percentage of C_{39}Me over C_{39}Et alkenones) may also indicate the contribution from Group II Isochrysidales or biosynthesis genes. Similarly, alkenone profiles in samples from Punta Grande/Punta Piccola sections (2.6–3.6 Ma) suggest production from both Group II (presence of extended C_{41} alkenones) and Group III (relatively high percentage of C_{38}Me alkenones over C_{38}Et alkenones) Isochrysidales (Plancq et al., 2015). More targeted genetic studies may help resolve the evolutionary process of alkenone productions in the Isochrysidales.

3.5. Alkenone temperature calibrations for I. nuda and I. litoralis

Numerous studies have provided relationships between alkenone unsaturation indices and growth temperature for various species or strains of Isochrysidales in culture experiments (Conte et al., 1998; Nakamura et al., 2014; 2016; Zheng et al., 2016; Araie et al., 2018). However, this is the first time that *I. nuda* and *I. litoralis* have been cultured to evaluate alkenone production.

3.5.1. Temperature calibrations of $U^{K'}_{41}$ and $U^{K'}_{42}$

Temperature calibrations for C_{41} ($U^{K'}_{41}$) and C_{42} ($U^{K'}_{42}$) alkenones were established for *I. nuda* (Fig. 3a). Because we only found $C_{41:3}$Me alkenone in *I. litoralis*, corresponding calibrations couldn't be established for this species. *I. nuda* displayed unusual behaviors: between 4 °C and 15 °C, $U^{K'}_{41}$ and $U^{K'}_{42}$ indices changed little, but showed a strong linear increasing trend with temperature from 15 °C to 25 °C. Similar behavior (i.e., little change when the temperature is below 15/10 °C) was also observed for alkenoate indices (U^{E}_{36Et}, $U^{E'}_{36Et}$, $U^{E''}_{36Et}$, U^{E}_{36Me}, $U^{E'}_{36Me}$, $U^{E''}_{36Me}$) of *I. nuda* (Supplementary Fig. S5). The only temperature calibration for C_{41}Me and C_{42}Et alkenones before this work was performed on strain *Sh 1* isolated from Lake Snakehole (Araie et al., 2018). Similarly, their calibrations of $U^{K'}_{41}$ and $U^{K'}_{42}$ (as well as alkenoate indices) showed little changes below 10 °C, but displayed strong linear increasing trends at higher temperatures. Therefore, the degree of unsaturation of C_{41}Me and C_{42}Et alkenones and alkenoates produced by *I. nuda* and closely related Group II species may only be reliable temperature proxies in relatively warm environments.

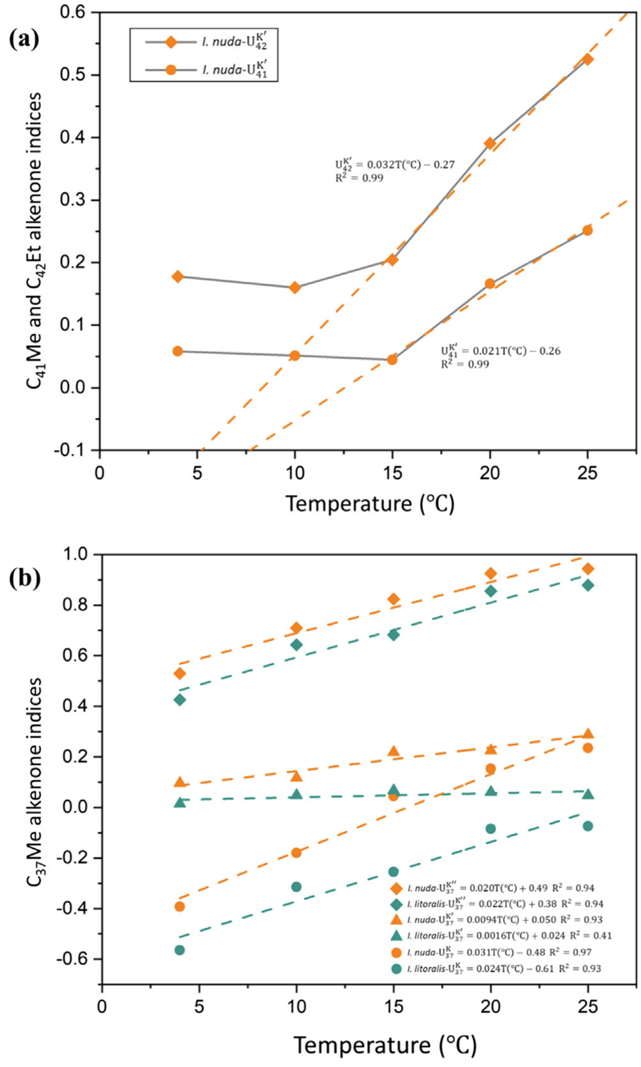

Fig. 3. (a) Temperature calibrations of $U^{K'}_{41}$ and $U^{K'}_{42}$ for *I. nuda* (RCC1207) from 4 to 25 °C in f/2 medium; (b) Temperature calibrations of U^{K}_{37}, $U^{K'}_{37}$ and $U^{K''}_{37}$ for *I. nuda* (RCC1207) and *I. litoralis* (AC18) from 4 °C to 25 °C in f/2 medium.

3.5.2. Temperature calibrations for C_{37}Me, C_{38}Et alkenones

Fig. 3b shows the calibrations of C_{37} alkenone unsaturation indices for *I. nuda* and *I. litoralis* against growth temperatures. We observed a similar phenomenon as previously reported by Zheng et al. (2016), that $U^{K''}_{37}$ and U^{K}_{37} displayed stronger linear relationships with growth temperatures (4 °C to 25 °C) than $U^{K'}_{37}$ in both species. The poorest linearity was observed for $U^{K'}_{37}$ of *I. litoralis*, which displayed very low temperature sensitivity (0.0016) and low $R^2 = 0.41$. The stronger linear relationship of double prime ($U^{K''}_{38Et}$) and no prime (U^{K}_{38Et}) indices over single prime indices ($U^{K'}_{38Et}$) could also be observed for C_{38}Et alkenones for *I. nuda* and *I litoralis* (Supplementary Table S2). Zheng et al. (2016) proposed that Group II Isochrysidales primarily use tri and tetra unsaturated alkenones to adapt to different environmental temperatures and that di-unsaturated alkenones are biosynthetic byproducts of this adaptation: our results here from *I. nuda* and *I. litoralis* further support this proposal. Interestingly, we found $U^{K''}_{37}$ index values of *I. nuda* and *I. litoralis* had similar temperature sensitivities as the closely related strain *Sh 1* grown in culture (slopes = 0.020 for *I. nuda*, 0.022 for *I. litoralis* and 0.026 for *Sh 1*), but were significantly different to the more distantly related *R. lamellosa* (slope = 0.032), *I. galbana* (slope = 0.015) and *T. lutea* (slope = 0.0011) (Araie et al., 2018; Zheng et al., 2019).

3.6. Influence of nutrient concentrations on the production of alkenones for I. nuda and I. litoralis

We performed preliminary experiments to study nutrient effects on alkenone productions for *I. nuda* and *I. litoralis*. At lower nutrient concentration (when the growth medium changed from f/2 to f/20), both *I. nuda* and *I. litoralis* produced higher percentages of C_{41}Me and C_{42}Et relative to C_{37}Me alkenones (Fig. 4a and b). In *I. nuda*, relative to C_{37} alkenones, alkenones with 38 to 42 carbon atoms all increased in abundances at lower nutrient level (17% increase for C_{38}Et, 403% increase for C_{41}Me and C_{42}Et). A similar trend was also observed for *I. litoralis* starting from C_{39}Me alkenones (but a slight decrease for C_{38}Et alkenones). Alkenone concentrations in each species increased from 0.8 pg/cell to 1.8 pg/cell for *I. nuda* and from 2.3 pg/cell to 4.6 pg/cell for *I. litoralis* (Supplementary Table S1). The increased production of alkenones with longer chain lengths and higher alkenone concentrations per cell under lower nutrient concentrations support the proposal that alkenones function as energy storage lipids and are produced in larger quantities when nutrient levels decrease (Bakku et al., 2018).

I. nuda and *I. litoralis* also showed increases in the degree of alkenone unsaturation with lower nutrient concentrations, which would lead to a decrease of alkenone index values and corresponding reconstructed temperatures (Fig. 4c–d). Among the three C_{37} alkenone indices examined, U^{K}_{37} displayed the largest decrease of index values (0.16 for *I. nuda*, 0.08 for *I. litoralis*), followed by $U^{K'}_{37}$ (0.08 for *I. nuda*, 0.05 for *I. litoralis*), and the smallest decrease in $U^{K''}_{37}$ (0.07 for *I. nuda* and 0.03 *for I. litoralis*). Because of the smaller slope in calibrations of U^{K}_{37} than that of U^{K}_{37}, reconstruction using $U^{K'}_{37}$ would instead decrease the inferred temperature by the largest quantity (8.9 °C for *I. nuda* and 32.4 °C for *I. litoralis*). In contrast, $U^{K''}_{37}$ had the smallest decrease of index values and inferred temperatures (3.7 °C for *I. nuda* and 1.3 °C for *I. litoralis*) when the growth medium changed from f/2 to f/20, suggesting that $U^{K''}_{37}$ is the least sensitive to nutrient manipulations. Overall, our data further support the use of $U^{K''}_{37}$ for paleotemperature reconstructions over U^{K}_{37} and $U^{K'}_{37}$ for Group II Isochrysidales (Zheng et al., 2016).

The decrease in $U^{K'}_{37}$ value at a lower nutrient level was previously observed in phosphate-limited culture experiments of *I. galbana* (Versteegh et al., 2001). In contrast, the limitation of nitrogen (nitrate and ammonium) was reported to have no significant influence on $U^{K'}_{37}$ value for *I. galbana* and *E. huxleyi* (Popp et al., 1998; Versteegh et al., 2001; Bakku et al., 2018). The difference in previously reported nutrient effects on alkenone unsaturation indices may reflect different roles of nitrogen and phosphorus in alkenone biosynthesis and different nutrient sensitivities for different Isochrysidales species. We note that nutrient effects on alkenone unsaturation indices are not observed in natural ocean surface sediment samples across large latitude ranges (Müller et al., 1998). More studies on natural alkenone samples from lacustrine and coastal regions would be helpful in further understanding the degree of influence on temperature reconstructions caused by nutrient effects for Group II species.

3.7. C_{41}Me and C_{42}Et alkenones in Lake Balikun and Lake Alahake and phylogenetic analysis

We have previously reported the occurrence of C_{41}Me and C_{42}Et alkenones in two hypersaline lakes (Balikun and Alahake) in north-

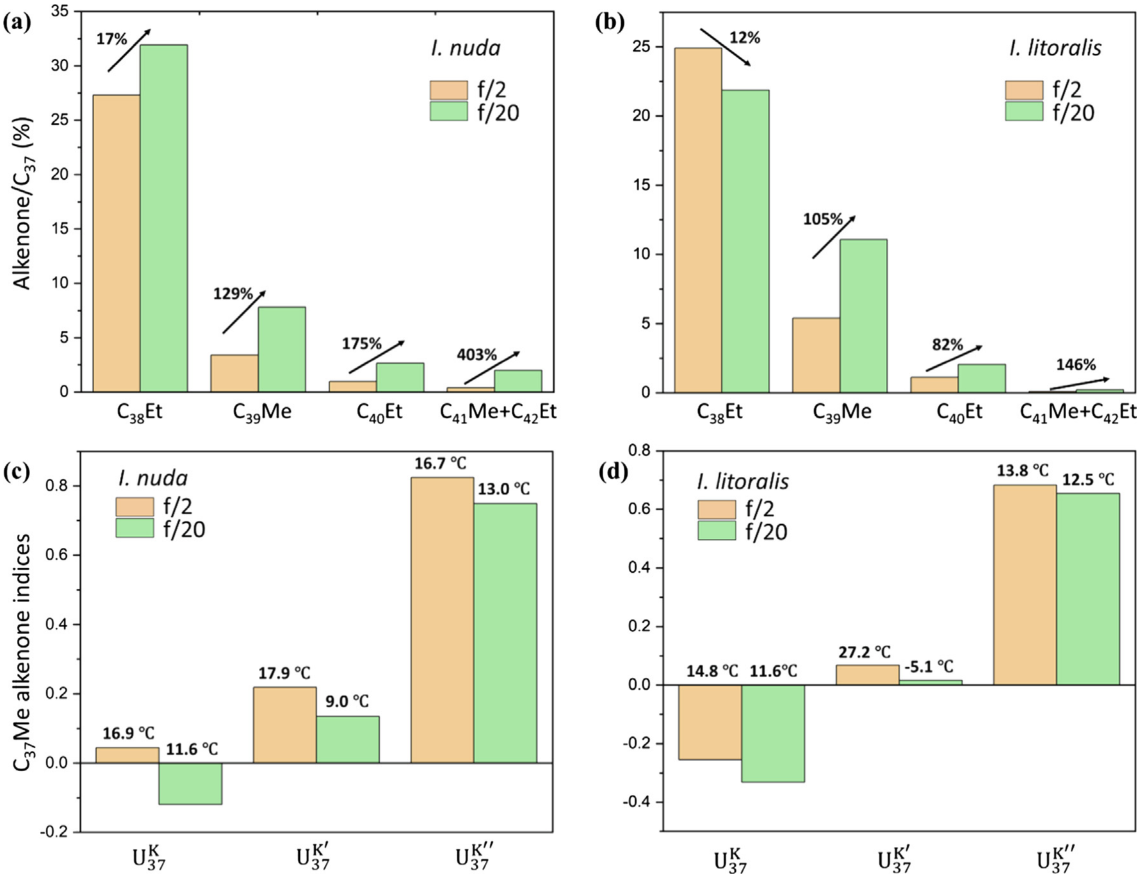

Fig. 4. Change of relative chain length distributions of alkenones (expressed as percentages relative to C_{37} alkenones) for *I. nuda* (RCC1207) (a) and *I. litoralis* (AC18) (b) from f/2 to f/20 medium. Change of index values and reconstructed temperatures using U^{K}_{37}, $U^{K'}_{37}$ and $U^{K''}_{37}$ for *I. nuda* (RCC1207) (c) and *I. litoralis* (AC18) (d) from f/2 to f/20 medium.

western China (Zhao et al., 2014). In this study, we re-examined newly collected surface sediments from these two lakes for alkenones and sequenced 18S rDNA to determine Isochrysidales species producing C_{41}Me and C_{42}Et alkenones. The newly collected sediment samples from Lake Balikun and Lake Alahake contained 3.2% and 5.6% C_{41}Me and C_{42}Et alkenones, respectively (Fig. 6a). All Isochrysidales sequences recovered in Lake Balikun belonged to Group II Isochrysidales, with 22 sequences assigned to an OTU closely related to strain *Sh 1*/*Sh 2* in Canadian Lake Snakehole, *I. nuda* and *I. litoralis* (Fig. 5), two sequences were similar to uncultured OTU7 haptophyte from Lake George, and five sequences were similar to *R. lamellosa*. No Isochrysidales sequences were recovered from Lake Alahake, probably due to poor DNA preservation in this lake. Factors affecting DNA preservation in Lake Balikun and Lake Alahake may include temperature (Lake Alahake's mean annual temperature, 5.02 °C, is higher than that of Lake Balikun, 1.75 °C), and different redox conditions in the bottom water (e.g., Corinaldesi et al., 2008).

The dominance of Isochrysidales sequences closely related to *I. nuda* as well as the occurrence of C_{41}Me and C_{42}Et alkenones in Lake Balikun and Lake Snakehole indicate that *I. nuda* (or closely related Isochrysidales) is most likely the dominant producer for C_{41}Me and C_{42}Et alkenones in saline lakes. While other Group II Isochrysidales species also produce C_{41}Me and C_{42}Et alkenones, *I. nuda* generally produces these extended-chain alkenones three times more than other Group II Isochrysidales (Fig. 2a, Supplementary Table S1). In the absence of *I. nuda* in saline lakes, detection of C_{41}Me and C_{42}Et alkenones would require injecting highly concentrated samples into GC-FID and GC–MS after extensive chromatographic cleaning to remove interfering compounds.

With the assumption that *I. nuda* (or closely related Isochrysidales) is the predominant Isochrysidales producing alkenones (especially C_{41}Me and C_{42}Et) in Lake Balikun and Lake Alahake, we can test how well our *I. nuda* culture temperature calibrations match with environmental temperatures. Fig. 6b shows the reconstructed temperatures usingU^{K}_{37}, $U^{K'}_{37}$, $U^{K''}_{37}$, U^{K}_{38Et}, $U^{K'}_{38Et}$, $U^{K''}_{38Et}$, $U^{K'}_{41}$ and $U^{K'}_{42}$ for Lake Balikun and Lake Alahake. We found temperatures based on extended C_{41}Me alkenone indices in both lakes matched warm-season temperatures (Fig. 6b). In contrast, reconstructions with $U^{K'}_{37}$ and $U^{K'}_{38Et}$ would yield unrealistic low temperatures. In Lake Alahake, $U^{K'}_{41}$-inferred temperature (15.7 °C) was similar to $U^{K''}_{37}$-inferred temperature (18.6 °C) and $U^{K''}_{38Et}$-inferred temperature (20.6 °C), and close to monthly air temperature from May to September (15.3–22.9 °C). On the other hand, $U^{K''}_{37}$-inferred temperature (5.3 °C) and $U^{K''}_{38Et}$-inferred temperature (–5.0 °C) were significantly lower than the $U^{K'}_{41}$-inferred temperature (16.9 °C) in Lake Balikun. C_{37} alkenones are produced in large quantities by all Isochrysidales species in Lake Balikun and Lake Alahake, whereas C_{41}Me and C_{42}Et alkenones are likely mainly produced by *I. nuda* (or closely related Isochrysidales). Different Group II Isochrysidales species may grow in different seasons and have different temperature calibrations (Theroux et al., 2020), complicating the use of C_{37} alkenones for temperature reconstructions. Therefore, in a relatively warm environment (>15 °C), reconstructions using $U^{K'}_{41}$ and $U^{K'}_{42}$ should be capable of reducing the effect of mixed alkenone productions and yielding records mainly reflecting the bloom seasons of dominant extended alkenone producers.

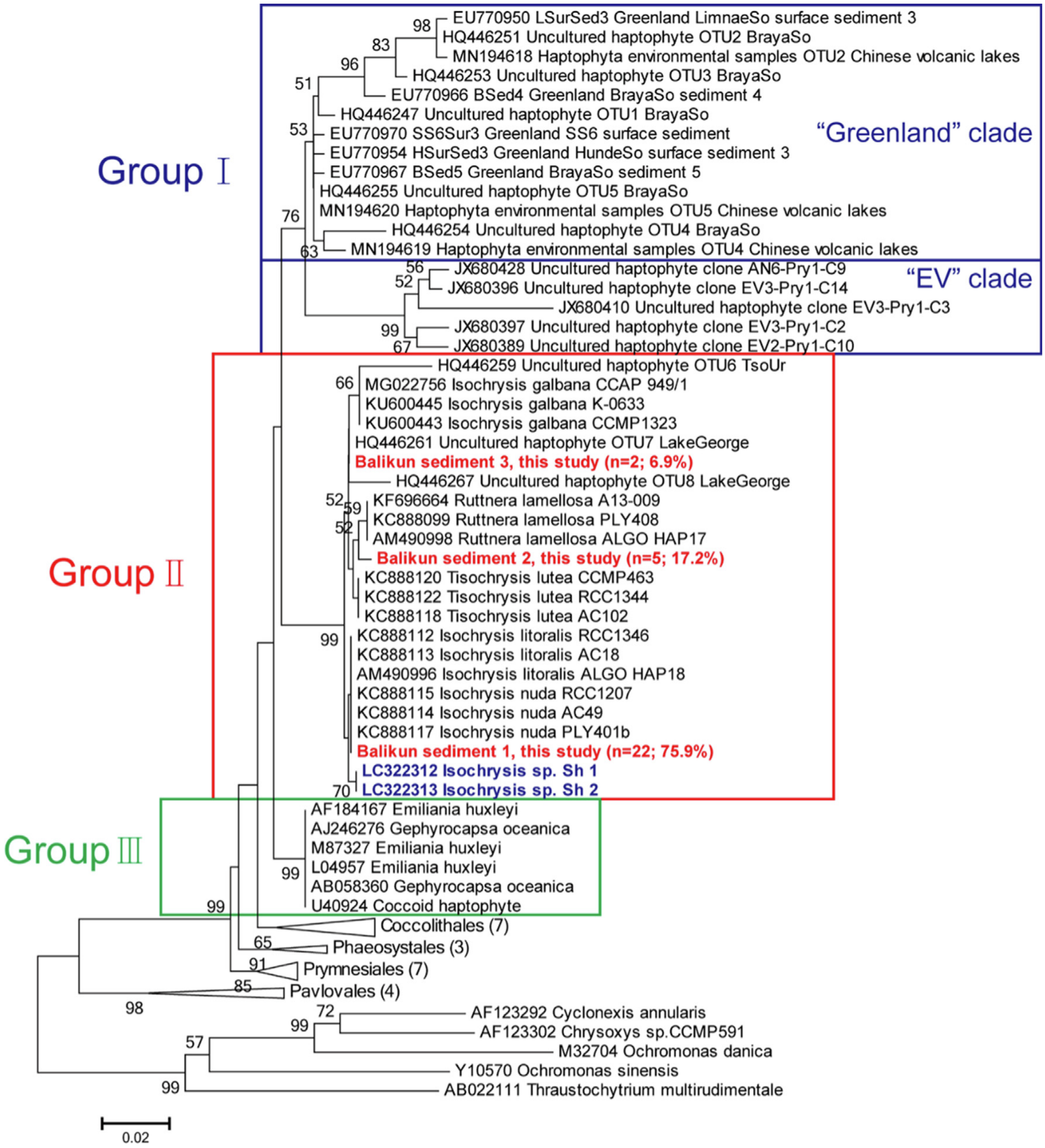

Fig. 5. Consensus neighbor-joining phylogenetic tree depicting 18SrRNA gene-inferred relatedness of haptophytes. Groups I, II and III Isochrysidales clades are labeled after Theroux et al. (2010). Greenland phylotypes on the tree include sequences recovered from freshwater lakes in Greenland (D'Andrea et al., 2006; Theroux et al., 2010) and volcanic lakes in northeastern China (Yao et al., 2019). EV phylotypes include sequences recovered from freshwater lakes in France (Simon et al., 2013).

4. Conclusions

C_{41}Me and C_{42}Et alkenones were found in all five Group II Isochrysidales species including *I. nuda, I. litoralis, R. lamellosa*, *I. galbana* and *T. lutea*, but not in Group III species *E. huxleyi* and *G. oceanica* nor in Group I environmental samples. Our data suggest that C_{41}Me and C_{42}Et alkenones are specific biomarkers for Group II Isochrysidales. Production of C_{41}Me and C_{42}Et alkenones varied among different Group II species with *I. nuda* having the highest production (up to 2% relative to C_{37} alkenones). In *I. nuda*, the relative percentages of C_{41}Me and C_{42}Et over C_{37}Me alkenones at 10 °C and 15 °C were lower than those at 4, 20 and 25 °C. *T. lutea* was only found to produce C_{41}Me and C_{42}Et alkenones in one culture at 25 °C but not at lower growth temperatures. This finding corroborates a previous study (Zheng et al., 2019), showing that *T. lutea* displays more Group II-like characteristics at higher temperatures, but more Group III-like features at lower temperatures.

The presence of C_{41}Me and C_{42}Et alkenones in sediment samples from Blake-Bahama Basin (~95 Ma), Bass River (~41 Ma) and Punta Grande/Punta Piccola sections (2.6–3.6 Ma) indicates alkenone production from Group II Isochrysidales or expression of Group II-type biosynthesis genes. Combined with other published alkenone profiles in sediments of the Cretaceous and early Eocene and evidence from rRNA-based molecular phylogenies, we hypothesize that Group II alkenone biosynthesis genes may have evolved earlier than those in Group III Isochrysidales.

$U_{41}^{K'}\text{and}U_{42}^{K'}$ in *I. nuda* displayed linear response towards temperatures from 15 °C to 25 °C, but changed little at lower temperatures. Our culture data from *I. nuda* and *I. litoralis* demonstrated that $U_{37}^{K''}$ $(\mathit{and}U_{38Et}^{K''})$ had greater linearity vs growth temperatures

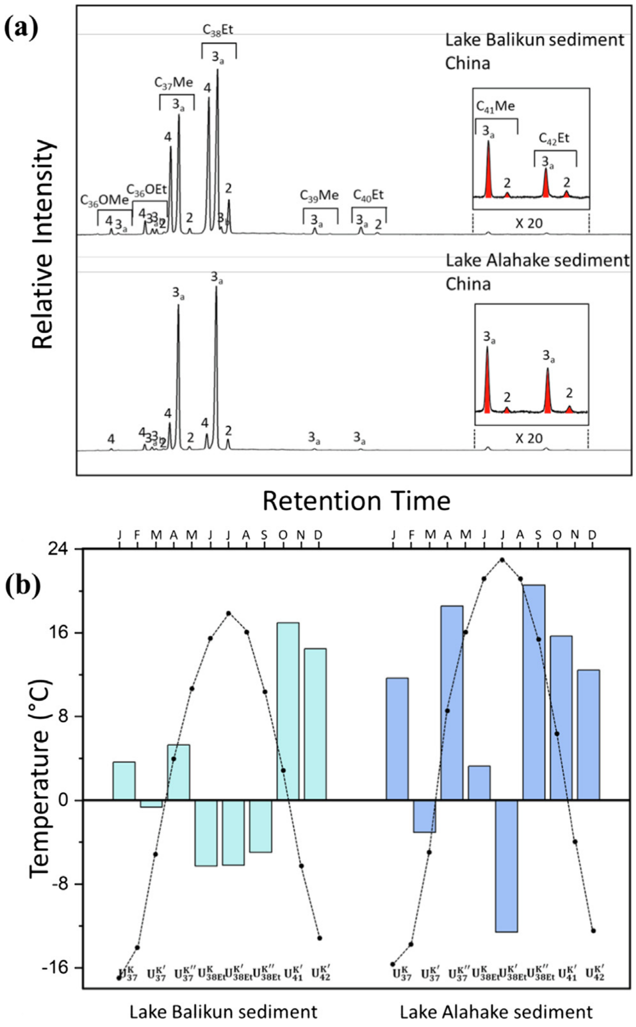

Fig. 6. (a) Gas chromatograms showing the distribution of alkenones and alkenoates of newly collected surface sediments from Lake Balikun and Lake Alahake after purified on a silver-thiolate column (Wang et al., 2019b). (b) Average monthly air temperature (1970–2000) and reconstructed temperatures using index values of U^{K}_{37}, $U^{K'}_{37}$, $U^{K''}_{37}$, U^{K}_{38Et}, $U^{K'}_{38Et}$, $U^{K''}_{38Et}$, $U^{K'}_{41}$ and $U^{K'}_{42}$ for Lake Balikun and Lake Alahake with corresponding calibrations of *I. nuda* (RCC1207). Calibrations of *I. nuda* (RCC1207) were selected because *I. nuda* (RCC1207) is more closely related to the main alkenone producer in Lake Balikun than strain *Sh 1* and calibrations of $U^{K'}_{41}$ and $U^{K'}_{42}$ were established for *I. nuda* (RCC1207) (but not for *I. litoralis* (AC18)).

than $U^{K'}_{37}$ ($U^{K'}_{38Et}$), consistent with previous findings from other Group II species (Zheng et al., 2019). Preliminary culture experiments also showed that $U^{K''}_{37}$ appeared to be less influenced than $U^{K'}_{37}$ under different nutrient concentrations. Our results reinforce the necessity of using double prime alkenone unsaturation indices for paleo-temperature reconstructions for Group II species.

Alkenone data (as well as DNA data in Lake Balikun) suggest that *I. nuda* (or closely related Isochrysidales) was the dominant Group II Isochrysidales in Lake Balikun and Lake Alahake. We found temperatures based on extended alkenone indices in both lakes matched warm season temperatures, and observed a significant difference in reconstructed temperatures with $U^{K''}_{37}$ and $U^{K'}_{41}$ indices from surface sediment of Lake Balikun. Our results suggest that temperature reconstructions using $U^{K'}_{41}$ and $U^{K'}_{42}$ indices in saline lakes could reduce the effect of mixed alkenone production from different Isochrysidales species and yield the most robust temperature reconstructions for relatively warm environments (>15 °C).

Declaration of Competing Interest

The authors declare that they have no known competing financial interests or personal relationships that could have appeared to influence the work reported in this paper.

Acknowledgments

This work was supported by the United States National Science Foundation awards to Y.H. (EAR-1122749, PLR-1503846, EAR-1502455; EAR-1762431). We would like to thank Fred Jackson, Tyler Kartzinel, Michele Grego, Leslie Murphy, Nicholas Vasques and Jacob Sullivan for their assistance during culture growth experiments. We are also grateful for the comments from Dr. Julien Plancq and an anonymous reviewer which helped us improve the manuscript.

Appendix A. Supplementary data

Supplementary data to this article can be found online at https://doi.org/10.1016/j.orggeochem.2020.104081.

Associate Editor–**George Wolff**

References

Araie, H., Nakamura, H., Toney, J.L., Haig, H.A., Plancq, J., Shiratori, T., Leavitt, P.R., Seki, O., Ishida, K., Sawada, K., Suzuki, I., Shiraiwa, Y., 2018. Novel alkenone-producing strains of genus *Isochrysis* (Haptophyta) isolated from Canadian saline lakes show temperature sensitivity of alkenones and *alkenoates*. *Organic Geochemistry* 121, 89–103.

Bakku, R.K., Araie, H., Hanawa, Y., Shiraiwa, Y., Suzuki, I., 2018. Changes in the accumulation of alkenones and lipids under nitrogen limitation and its relation to other energy storage metabolites in the haptophyte alga *Emiliania huxleyi CCMP 2090*. *Journal of Applied Phycology* 30, 23–36.

Bendif, E.M., Probert, I., Schroeder, D.C., de Vargas, C., 2013. On the description of *Tisochrysis lutea* gen. nov. sp. nov. and *Isochrysis nuda* sp. nov. in the Isochrysidales, and the transfer of *Dicrateria* to the Prymnesiales (Haptophyta). Journal of Applied Phycology 25, 1763–1776.

Bendle, J., Rosell-Melé, A., 2007. High-resolution alkenone sea surface temperature variability on the North Icelandic Shelf: implications for Nordic Seas palaeoclimatic development during the Holocene. The Holocene 17, 9–24.

Brassell, S.C., Eglinton, G., Marlowe, I.T., Pflaumann, U., Sarnthein, M., 1986. Molecular stratigraphy: a new tool for climatic assessment. Nature 320, 129–133.

Brassell, S.C., Dumitrescu, M., The ODP Leg 198 Shipboard Scientific Party, 2004. Recognition of alkenones in a lower Aptian porcellanite from the west-central Pacific. Organic Geochemistry 35, 181–188.

Brassell, S.C., 2014. Climatic influences on the Paleogene evolution of alkenones. Paleoceanography 29, 255–272.

Conte, M.H., Thompson, A., Lesley, D., Harris, R.P., 1998. Genetic and physiological influences on the alkenone/alkenoate versus growth temperature relationship in *Emiliania huxleyi* and *Gephyrocapsa oceanica*. Geochimica et Cosmochimica Acta 62, 51–68.

Coolen, M.J.L., Muyzer, G., Rijpstra, W.I.C., Schouten, S., Volkman, J.K., Sinninghe Damsté, J.S., 2004. Combined DNA and lipid analyses of sediments reveal changes in Holocene haptophyte and diatom populations in an Antarctic lake. Earth and Planetary Science Letters 223, 225–239.

Corinaldesi, C., Beolchini, F., Dell'Anno, A., 2008. Damage and degradation rates of extracellular DNA in marine sediments: implications for the preservation of gene sequences. Molecular Ecology 17, 3939–3951.

D'Andrea, W.J., Huang, Y., 2005. Long chain alkenones in Greenland lake sediments: Low δ^{13}C values and exceptional abundance. Organic Geochemistry 36, 1234–1241.

D'Andrea, W.J., Lage, M., Martiny, J.B.H., Laatsch, A.D., Amaral-Zettler, L.A., Sogin, M. L., Huang, Y., 2006. Alkenone producers inferred from well-preserved 18S rDNA in Greenland lake sediments. Journal of Geophysical Research 111, G03013.

de Bar, M.W., Rampen, S.W., Hopmans, E.C., Sinninghe Damsté, J.S., Schouten, S., 2019. Constraining the applicability of organic paleotemperature proxies for the last 90 Myrs. Organic Geochemistry 128, 122–136.

Dillon, J.T., Longo, W.M., Zhang, Y., Torozo, R., Huang, Y., 2016. Identification of double-bond positions in isomeric alkenones from a lacustrine haptophyte. Rapid Communications in Mass Spectrometry 30, 112–118.

Epstein, B.L., D'Hondt, S., Hargraves, P.E., 2001. The possible metabolic role of C_{37} alkenones in *Emiliania huxleyi*. Organic Geochemistry 32, 867–875.

Farrimond, P., Eglinton, G., Brassell, S.C., 1986. Alkenones in Cretaceous black shales, Blake-Bahama Basin, western North Atlantic. Organic Geochemistry 10, 897–903.

Fick, S.E., Hijmans, R.J., 2017. WorldClim 2: new 1-km spatial resolution climate surfaces for global land areas. International Journal of Climatology 37, 4302–4315.

Guillard, R.R.L., 1975. Culture of Phytoplankton for Feeding Marine Invertebrates. In: Smith, W.L., Chanley, M.H. (Eds.), Culture of Marine Invertebrate Animals. Plenum Press, New York, USA, pp. 26–60.

Harada, N., Shin, K.H., Murata, A., Uchida, M., Nakatani, T., 2003. Characteristics of alkenones synthesized by a bloom of *Emiliania huxleyi* in the Bering Sea. Geochimica et Cosmochimica Acta 67, 1507–1519.

Kaiser, J., Wang, K.J., Rott, D., Li, G., Zheng, Y., Amaral-Zettler, L., Arz, H.W., Huang, Y., 2019. Changes in long chain alkenone distributions and Isochrysidales groups along the Baltic Sea salinity gradient. Organic Geochemistry 127, 92–103.

Longo, W.M., Dillon, J.T., Tarozo, R., Salacup, J.M., Huang, Y., 2013. Unprecedented separation of long chain alkenones from gas chromatography with a poly (trifluoropropylmethylsiloxane) stationary phase. Organic Geochemistry 65, 94–102.

Longo, W.M., Theroux, S., Gibin, A.E., Zheng, Y., Dillon, J.T., Huang, Y., 2016. Temperature calibration and phylogenetically distinct distributions for freshwater alkenones: Evidence from northern Alaskan lakes. Geochimica et Cosmochimica Acta 180, 177–196.

Longo, W.M., Huang, Y., Yao, Y., Zhao, J., Giblin, A.E., Wang, X., Zech, R., Haberzettl, T., Jardillier, L., Toney, J., Liu, Z.H., Krivonogov, S., Kolpakova, M., Chu, G.Q., D'Andrea, W.J., Harada, N., Nagashima, K., Sato, M., Yonenobu, H., Yamada, K., Gotanda, K., Shinozuka, Y., 2018. Widespread occurrence of distinct alkenones from Group I haptophytes in freshwater lakes: Implications for paleotemperature and paleoenvironmental reconstructions. Earth and Planetary Science Letters 492, 239–250.

Müller, P.J., Kirst, G., Ruhland, G., von Storch, I., Rosell-Melé, A., 1998. Calibration of the alkenone paleotemperature index U37K' based on core-tops from the eastern South Atlantic and the global ocean (60°N–60°S). Geochimica et Cosmochimica Acta 62, 1757–1772.

Nakamura, H., Sawada, K., Araie, H., Suzuki, I., Shiraiwa, Y., 2014. Long chain alkenes, alkenones and alkenoates produced by the haptophyte alga *Chrysotila lamellosa* CCMP1307 isolated from a salt marsh. Organic Geochemistry 66, 90–97.

Nakamura, H., Sawada, K., Araie, H., Shiratori, T., Ishida, K., Suzuki, I., Shiraiwa, Y., 2016. Composition of long chain alkenones and alkenoates as a function of growth temperature in marine haptophyte *Tisochrysis lutea*. Organic Geochemistry 99, 78–89.

O'Brien, C.L., Robinson, S.A., Pancost, R.D., Sinninghe Damsté, J.S., Schouten, S., Lunt, D.J., Alsenz, H., Bornemann, A., Bottini, C., Brassell, S.C., Farnsworth, A., Forster, A., Huber, B.T., Inglis, G.N., Jenkyns, H.C., Linnert, C., Littler, K., Markwick, P., McAnena, A., Mutterlose, J., Naafs, B.D.A., Püttmann, W., Sluijs, A., van Helmond, N.A.G.M., Vellekoop, J., Wagner, T., Wrobel, N.E., 2017. Cretaceous sea-surface temperature evolution: Constraints from TEX_{86} and planktonic foraminiferal oxygen isotopes. Earth-Science Reviews 172, 224–247.

Plancq, J., Grossi, V., Pittet, B., Huguet, C., Rosell-Melé, A., Mattioli, E., 2015. Multi-proxy constraints on sapropel formation during the late Pliocene of central Mediterranean (southwest Sicily). Earth and Planetary Science Letters 420, 30–44.

Popp, B.N., Kenig, F., Wakeham, S.G., Laws, E.A., Bidigare, R.R., 1998. Does growth rate affect ketone unsaturation and intracellular carbon isotopic variability in *Emiliania huxleyi*? Paleoceanography 13, 35–41.

Prahl, F.G., Wakeham, S.G., 1987. Calibration of unsaturation patterns in long-chain ketone compositions for paleotemperature assessment. Nature 330, 367–369.

Pujos-Lamy, A., 1977. Essai d'établissement d'une biostratigraphie du nannoplancton calcaire dans le Pleistocène de l'Atlantique Nord-oriental. Boreas 6, 323–331.

Raffi, I., Backman, J., Fornaciari, E., Pälike, H., Rio, D., Lourens, L.J., Hilgen, F., 2006. A review of calcareous nannofossil astrobiochronology encompassing the past 25 million years. Quaternary Science Reviews 25, 3113–3137.

Randlett, M.E., Coolen, M.J.L., Stockhecke, M., Pickarski, N., Litt, T., Balkema, C., Kwiecien, O., Tomonaga, Y., Wehrli, B., Schubert, C.J., 2014. Alkenone distribution in Lake Van sediment over the last 270 ka: influence of temperature and haptophyte species composition. Quaternary Science Reviews 104, 53–62.

Richter, N., Longo, W.M., George, S., Shipunova, A., Huang, Y., Amaral-Zettler, L., 2019. Phylogenetic diversity in freshwate–dwelling Isochrysidales haptophytes with implications for alkenone production. Geobiology 17, 272–280.

Rosell-Melé, A., Comes, P., 1999. Evidence for a warm Last Glacial Maximum in the Nordic seas or an example of shortcomings in U37K' and U37K to estimate low sea surface temperature? Paleoceanography 14, 770–776.

Schloss, P.D., Handelsman, J., 2005. Introducing DOTUR, a computer program for defining operational taxonomic units and estimating species richness. Applied and Environmental Microbiology 71, 1501–1506.

Shi, Q., Araie, H., Bakku, R.K., Fukao, Y., Rakwal, R., Suzuki, I., Shiraiwa, Y., 2015. Proteomic analysis of lipid body from the alkenone-producing marine haptophyte alga *Tisochrysis lutea*. Proteomics 15, 4145–4158.

Simon, M., López-García, P., Moreira, D., Jardillier, L., 2013. New haptophyte lineages and multiple independent colonizations of freshwater ecosystems. Environmental Microbiology Reports 5, 322–332.

Theroux, S., D'Andrea, W.J., Toney, J., Amaral-Zettler, L., Huang, Y., 2010. Phylogenetic diversity and evolutionary relatedness of alkenone-producing haptophyte algae in lakes: Implications for continental paleotemperature reconstructions. Earth and Planetary Science Letters 300, 311–320.

Theroux, S., Huang, Y., Toney, J.L., Andersen, R., Nyren, P., Bohn, R., Salacup, J., Murphy, L., Amaral-Zettler, L., 2020. Successional blooms of alkenone-producing haptophytes in Lake George, North Dakota: Implications for continental paleoclimate reconstructions. Limnology and Oceanography 65, 413–425.

Tzanova, A., Herbert, T.D., 2015. Regional and global significance of Pliocene sea surface temperatures from the Gulf of Cadiz (Site U1387) and the Mediterranean. Global and Planetary Change 133, 371–377.

Versteegh, G.J.M., Riegman, R., de Leeuw, J.W., Jansen, J.H.F.F., 2001. U37K' values for Isochrysis galbana as a function of culture temperature, light intensity and nutrient concentrations. Organic Geochemistry 32, 785–794.

Volkman, J.K., Eglinton, G., Corner, E.D.S., Forsberg, T.E.V., 1980. Long-chain alkenes and alkenones in the marine coccolithophorid *Emiliania huxleyi*. Phytochemistry 19, 2619–2622.

Wang, K.J., O'Donnell, J.A., Longo, W.M., Amaral-Zettler, L., Li, G., Yao, Y., Huang, Y., 2019a. Group I alkenones and Isochrysidales in the world's largest maar lakes and their potential paleoclimate applications. Organic Geochemistry 138, 103924.

Wang, L., Longo, W.M., Dillon, J.T., Zhao, J., Zheng, Y., Moros, M., Huang, Y., 2019b. An efficient approach to eliminate steryl ethers and miscellaneous esters/ketones for gas chromatographic analysis of alkenones and alkenoates. Journal of Chromatography A 1596, 175–182.

Weller, P., Stein, R., 2008. Paleogene biomarker records from the central Arctic Ocean (Integrated Ocean Drilling Program Expedition 302): Organic carbon sources, anoxia, and sea surface temperature. Paleoceanography 23, 15.

Yamamoto, M., Ficken, K., Baas, M., Bosch, H.J., de Leeuw, J.W., 1996. Molecular palaeontology of the earliest Danian at Geulhemmerberg (the Netherlands). Geologie En Mijnbouw 75, 255–267.

Yao, Y., Zhao, J., Longo, W.M., Li, G., Wang, X., Vachula, R.S., Wang, K.J., Huang, Y., 2019. New insights into environmental controls on the occurrence and abundance of Group I alkenones and their paleoclimate applications: evidence from volcanic lakes of northeastern China. Earth and Planetary Science Letters 527, 115792.

Zhao, J., An, C., Longo, W.M., Dillon, J.T., Zhao, Y., Shi, C., Chen, Y., Huang, Y., 2014. Occurrence of extended chain length C_{41} and C_{42} alkenones in hypersaline lakes. Organic Geochemistry 75, 48–53.

Zheng, Y., Huang, Y., Andersen, R.A., Amaral-Zettler, L.A., 2016. Excluding the di-unsaturated alkenone in the U37K index strengthens temperature correlation for the common lacustrine and brackish-water haptophytes. Geochimica et Cosmochimica Acta 175, 36–46.

Zheng, Y., Tarozo, R., Huang, Y., 2017. Optimizing chromatographic resolution for simultaneous quantification of long chain alkenones, alkenoates and their double bond positional isomers. Organic Geochemistry 111, 136–143.

Zheng, Y., Heng, P., Conte, M.H., Vachula, R.S., Huang, Y., 2019. Systematic chemotaxonomic profiling and novel paleotemperature indices based on alkenones and alkenoates: Potential for disentangling mixed species input. *Organic Geochemistry* 128, 26–41.